Quaternary International 459 (2017) 29–34

Contents lists available at ScienceDirect

Quaternary International

journal homepage: www.elsevier.com/locate/quaint

Northern South China Sea SST changes over the last two millennia and possible linkage with solar irradiance

Deming Kong [a, b, *], Gangjian Wei [c], Min-Te Chen [d, **], Shiyun Peng [a], Zhonghui Liu [b]

[a] Guangdong Province Key Laboratory for Coastal Ocean Variation and Disaster Prediction, College of Ocean and Meteorology, Guangdong Ocean University, Zhanjiang 524088, China
[b] Department of Earth Sciences, The University of Hong Kong, Hong Kong, China
[c] CAS Key Laboratory of Marginal Sea Geology, Guangzhou Institute of Geochemistry, Chinese Academy of Sciences, Guangzhou 510640, China
[d] Institute of Applied Geosciences, National Taiwan Ocean University, Keelung 20224, Taiwan

ARTICLE INFO

Article history:
Received 28 June 2017
Received in revised form
1 October 2017
Accepted 2 October 2017
Available online 16 October 2017

Keywords:
Alkenone
South China Sea
SST
2ka
Solar irradiance

ABSTRACT

High-resolution surface temperature records over the last two millennia are crucial to understanding the forcing and response mechanism of Earth's climate. Here we report a bidecadal-resolution sea surface temperature (SST) record based on long-chain alkenones in a gravity sediment core retrieved from the northern South China Sea. SST values varied between 26.7 and 27.5 °C, with a total variability ~1 °C over the last 2000 years. The general SST variation pattern matches well with total solar irradiance (TSI) changes. Relatively warm period between 800 and 1400 AD and cool period 1400-1850 AD could be identified, in agreement with the commonly defined periods of Medieval Warm Period and Little Ice Age. Within chronological uncertainty, notable short cooling events at 640-670 AD, 1030-1080 AD, 1260-1280 AD and 1420-1450 AD, coincide with large volcanic eruption events. The general coincidence of SST changes with TSI and volcanic eruption events suggests strong impact of external forcing on sea surface conditions in the studied area. In addition to the direct TSI changes, volcanic eruptions might have induced oceanic and atmospheric circulation adjustments which might be responsible for the short cooling events as revealed in the alkenone-SST record.

1. Introduction

Earth's surface temperature changes over the last two millennia have been crucial to understanding current global warming issues, and reconstructed at regional, continental, and global scales using proxy data from various archives (Mann, 2007). Many of the high-resolution data have been used to produce a global array of climate as part of the "2k Network" in the IGBP Past Global Changes (PAGES) project (Ljungqvist et al., 2012; Mann, 2007, 2008; Mann and Jones, 2003; Neukom and Gergis, 2012; Neukom et al., 2014; PAGES 2k Consortium, 2013; PAGES Ocean2k Working Group, 2012), as well as in the 4th and 5th IPCC Assessment Report. Now some concepts, such as the Medieval Warm Period (WMP) and Little Ice Age (LIA), are widely accepted as the common climatic features over the last two millennia. However, comparisons among high-resolution temperature records derived from different proxies show distinctly spatial discrepancies, particularly between land and ocean, northern and southern hemispheres (PAGES 2k Consortium, 2013). Indeed, even the most prominent epochs during the last two millennia, the WMP and LIA, do not have specific definitions in terms of their time span, suggesting no global synchronous temperature patterns (Mann, 2007; PAGES 2k Consortium, 2013). Studies on those discrepancies would be helpful to deciphering climatic forcing-response processes, which however requires adequate coverage of high-resolution temperature reconstructions from various environment settings.

The mostly used annually-resolved proxy data are from continental archives, such as tree rings (Anchukaitis et al., 2012; Liu et al., 2009; Wilson et al., 2016) and ice cores (Dahljensen et al., 1998; Kobashi et al., 2011). Marine archives like corals and giant clams could produce annual-resolution paleotemperatures, which are often too short in most cases, and therefore usually concatenated to produce longer temperature records at millennial scale

* Corresponding author. Guangdong Province Key Laboratory for Coastal Ocean Variation and Disaster Prediction, College of Ocean and Meteorology, Guangdong Ocean University, Zhanjiang 524088, China.
** Corresponding author.
E-mail addresses: kongdm@gdou.edu.cn (D. Kong), mtchen@ntou.edu.tw (M.-T. Chen).

https://doi.org/10.1016/j.quaint.2017.10.001
1040-6182/© 2017 Published by Elsevier Ltd.

(Cobb et al., 2003; Yan et al., 2015). Marine sediments with relatively high sedimentation rates could provide continuous, decadal-resolution temperature reconstructions based on the foraminifera Mg/Ca (Oppo et al., 2009), GDGTs (Wu et al., 2012) and long-chain alkenones (Ruan et al., 2015; Sicre et al., 2008; Zhao et al., 2006).

The unsaturation index of long-chain alkenones ($U^{K'}_{37}$) have been established as an useful proxy to reconstruct sea surface temperature (SST) (Conte et al., 2006; Müller et al., 1998; Sikes et al., 1997; Volkman et al., 1995), and thought to have better indication to the most surface temperature than other proxies (Smith et al., 2013). At longer timescale, $U^{K'}_{37}$-SSTs generally record climate changes driven by earth's orbital cycles (Liu and Herbert, 2004). At millennial to centennial scale, changes in the $U^{K'}_{37}$-SST are usually interpreted to respond to monsoon or oceanic circulation changes (Kong et al., 2014, 2015; Zhao et al., 2014; Zhao et al., 2006). With increasing resolution amount and number of alkenone-derived SST records, distinct differences have found between $U^{K'}_{37}$-SSTs in the coastal and open sea of northern South China Sea (SCS), particularly during the late Holocene (Kong et al., 2014; Wang et al., 1999b). Similar to the northern SCS, the general trend of many $U^{K'}_{37}$-SSTs records have been found to follow the increasing winter insolation through the Holocene in the tropical Pacific and Indian oceans (Leduc et al., 2010).

The impact of solar irradiance and volcanic eruptions on continental temperatures could be clearly identified from annual-to decadal-resolution records, and the two are considered as the main external forcings (Anchukaitis et al., 2012; Gao et al., 2008; Mann, 2007; PAGES 2k Consortium, 2013). In contrast, it is still unclear how SSTs were influenced by different forcing factors, partly due to lacking adequate continuous high-resolution SST records (PAGES Ocean2k Working Group, 2012).

Here, we have analyzed long-chain alkenones in the upper 45 cm of a gravity core NS02G, covering the last 2000 years. Our main objectives are to reconstruct a bidecadal-resolution SST record in the open sea of northern SCS, and assess the regional temperature response and potential forcing mechanisms.

2. Oceanographic settings

The study area is located in the northern South China Sea (SCS), largest marginal sea of the Western Pacific Ocean. The SCS is almost a semi-enclosed, connected to surrounding seas and oceans through 5 narrow straits in the south, Taiwan and Luzon Strait in the north. The Taiwan and Luzon Straits are the important channels for water and thermal exchange with East China Sea and Western Pacific. The current through the Luzon Strait is considered as an intrusion branch of the Kuroshio Current off east coast of Philippines (Hu et al., 2000; Xue et al., 2004).

The annual mean SST of the southern part is higher than 28 °C and included to the Western Pacific Warm Pool (WPWP, SST>28 °C). The northern SCS shows distinct seasonal patterns in the SST field (http://apdrc.soest.hawaii.edu/) under the influence of Asian monsoons and Kuroshio Current intrusion. In summer, SST distribution is nearly homogenous across the northern SCS, while in winter, coastal SST is much lower than the open sea. The temperature isotherms are almost parallel with the southern China coastal line. Generally, the SST distribution in the northern SCS is strongly modulated by the Asian summer and winter monsoons (Su, 2004).

3. Sampling and analytical methods

3.1. Sampling

A 4.6-meter gravity core NS02G (19.8° N, 113.9° E) was retrieved from the offshore continental slope at a water depth of 562 m in the northern SCS (Fig. 1) in April 2012, by Guangzhou Marine Geological Survey Bureau. Monthly SST at the NS02G location ranges from ~22 °C in winter to ~30 °C in summer with an annual mean at ~26.5 °C (http://www.esrl.noaa.gov/psd/data/timeseries/). The whole NS02G core consists of gray clay and is rich in foraminifera.

3.2. Chronology

The chronology of NS02G is based on accelerator mass spectrometry (AMS) ^{14}C ages of 14 planktonic foraminifera specimens. All the foraminifera samples except R01 used for ^{14}C dating are mixtures of *Globigerinoides ruber* and *Globigerinoides sacculifer*. The foraminifera were pretreated under standard procedure, and measured ^{14}C concentration at the Beta Analytic laboratory in Miami, USA. Among the results, 6 AMS ^{14}C ages have been published previously (Kong et al., 2014), other 8 new ages were measured in September, 2017.

Foraminifera species picked from the core top sediment sample R01 (0–3 cm) is *Globigerinoides ruber* (white). Measured ^{14}C concentration of R01 is 108.2 ± 0.4 percent of modern carbon (pMC, 1950 AD as reference). It suggests that the foraminifers were living after the year 1950 AD. Some colored foraminifers with fragile spines were observed in sample R01 under the microscope, suggesting the core top sediment is quite "fresh". The ^{210}Pb dating results on core NS02G have been reported by Kong et al. (2014). The excess ^{210}Pb concentration of the top 1 cm is 669 Bq/kg, and drops fast to about zero at ~3 cm. This confirms the young ^{14}C age of sample R01, and suggests the surface sediment had not been disturbed. Based on the ^{14}C and ^{210}Pb results, the depth 2 cm in the core was set as 0 cal yr BP, and the age above 2 cm was roughly calculated as after 1950 AD.

The measured ^{14}C ages of all the foraminifera samples (except R01) were calibrated using Marine13 dataset (Reimer et al., 2013) and CALIB 7.04 program with 400 years reservoir (ΔR = 0)

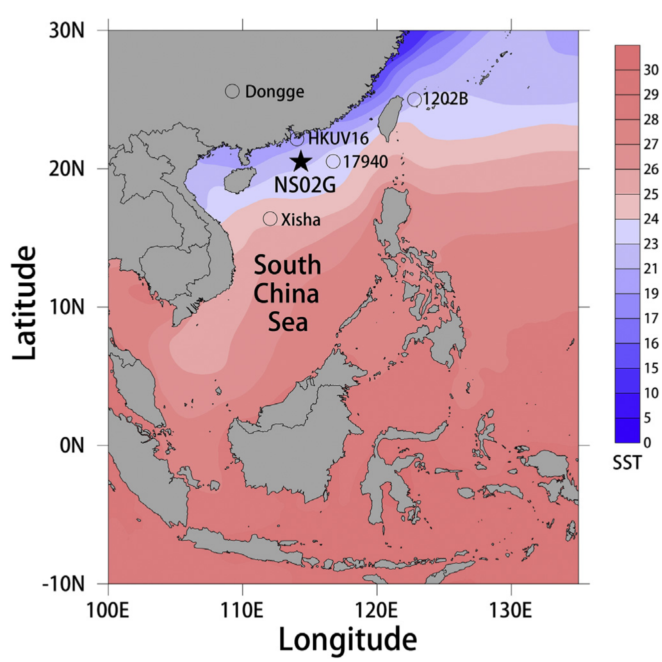

Fig. 1. Map of study area and sampling site NS02G (black star). Black circles denotes studied sites cited in this paper. The color contour is 30-years (1980-2010) averaged January SST (http://apdrc.soest.hawaii.edu/las/v6/constrain?var=962). (For interpretation of the references to colour in this figure legend, the reader is referred to the web version of this article).

correction (Wang et al., 1999a). As the sedimentation rate of the whole core seems quite constant, polynomial (n = 2) fitting between all the calibrated ^{14}C ages and depth (D in cm) was adopted to establish the age model (Fig. 2). The fitting result is: age (a cal BP) = −0.0145*D^2+46.898*D-112.42 (R^2 = 0.9978). Ages of the whole core were calculated from this equation.

3.3. Alkenone analysis

The core NS02G were subsampled at every 0.5 cm interval. About 90 samples in the top 45 cm of NS02G were used for long-chain alkenone analysis. The pretreatment and analysis methods, along with ~20 data points, have been reported by Kong et al. (2014). The SST was calculated using the SCS $U^{K'}_{37}$-SST calibration equation: $U^{K'}_{37}$ = 0.031SST+0.092 (Pelejero and Grimalt, 1997). Replicate injections of standards in different batches show analytical errors less than 0.3 °C for the calculated SST.

4. Results

A centennial-resolution $U^{K'}_{37}$-SST record over the past 8000 years from the core NS02G, analyzed at 2.5 cm interval, has been reported previously (Kong et al., 2014). The increased data resolution, subsampled at 0.5 cm interval, better characterizes SST changes over the last 2 millennia. Based to our current chronology, there exist 90 data points after 0 AD, yielding an average resolution of every ~22 years per sample (Fig. 3). Such a resolution, although still not comparable with some terrestrial temperature records, is quite decent as compared to previous alkenone-derived SST records in the northern SCS (Shintani et al., 2008; Wang et al., 1999b; Wei et al., 2007). To date, the calibration equation ($U^{K'}_{37}$=0.031SST+0.092) by Pelejero and Grimalt (1997) rather than the global core top equation by (Müller et al., 1998) is used in most studies of $U^{K'}_{37}$-based paleotemperature reconstructions in the SCS. To keep the SST comparable with previous SST records in the SCS, the equation $U^{K'}_{37}$ = 0.031SST+0.092 is used to calculate SST in this study.

The calculated SST of NS02G over the last 2000 years ranges from 26.7 to 27.5 °C, averaged at 27.04 °C (Fig. 3). The SST curve exhibits a "W" shape without a significant overall increasing or decreasing trend. Though the variability is small, several relatively warm and cool periods could be identified. The SST decreased slightly from 0 to ~620 AD, followed by an abrupt cooling by ~0.3 °C at 640-670 AD. Then it increased to the warmest point 27.5 °C at ~970 AD. It experienced a relatively warm period between 900-1380 AD, which interrupted by two significant cooling episodes at 1030-1080 AD and ~1270 AD. After a fast drop to 26.7 °C at 1430 AD, SST has gradually increased to 27.3 °C at the topmost, but has not exceeded the peak values at ~970 AD. Generally, the SST record is characterized with a warm epoch during ~900-1380 AD and several abrupt cooling events at 640–670, 1030–1080, 1260–1280, 1420–1450 and ~1550 AD, respectively.

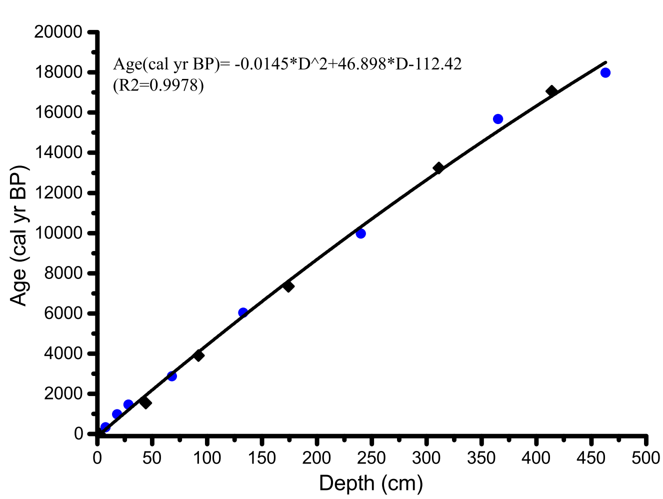

Fig. 2. Polynomial fitting (n=2) of all 14 calibrated AMS ^{14}C ages with the center depth (in cm) that the foraminifera picked from. The fitting result is :Age(cal yr BP)=-0.0145*D^2+46.898*D-112.42 (R^2=0.9978). Black diamonds denote ages published in Kong et al. (2014). Blude dots are the ages measured in September, 2017. (For interpretation of the references to colour in this figure legend, the reader is referred to the web version of this article).

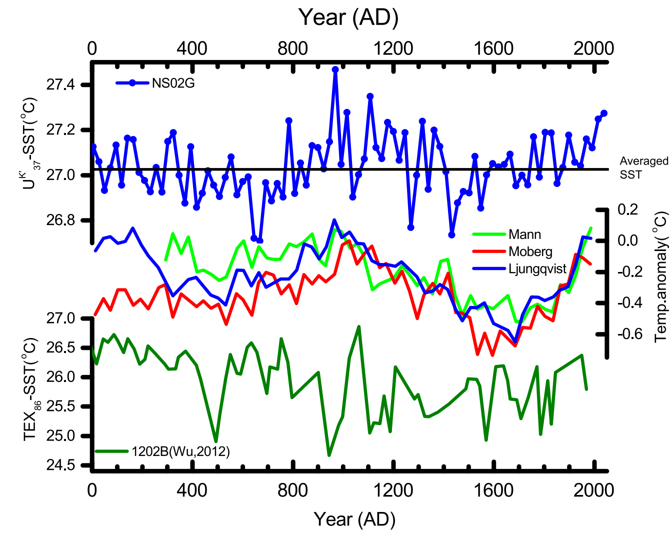

Fig. 3. $U^{K'}_{37}$-SST of core NS02G (blue dots) since 0 AD with average reference(solid black line). Three combined contiental temperature anomalies are from a review by Ahmed et al.,2013. Green line (Mann, 2008); blue line (Ljungqvist, 2010); red line (Moberg et al., 2005); deep green line is TEX_{86}-SST from core 1202B (Wu et al., 2012). (For interpretation of the references to colour in this figure legend, the reader is referred to the web version of this article).

5. Discussion

5.1. Validation of the reconstructed SST

To assess potential systematic and analytical errors in the SST reconstruction, calculated SST of NS02G was compared with core 17940 (Wang et al., 1999b), which is ~200 km east to the NS02G core location. The $U^{K'}_{37}$-SST is calculated using the same equation by Pelejero and Grimalt (1997). The SST of NS02G over the last 2000 years range between 26.7 and 27.5 °C, with an average at 27.04 °C and variability ~1 °C. The average SST is very close to the averaged SST (26.98 °C) at Core 17940 over the last 2 millennia (Wang et al., 1999b). The variability was slightly higher in NS02G, possibly due to higher sampling resolution. The observed range of SST changes over the last 2 millennia also exceeds the typical analytical error in our lab, up to 0.3 °C, based on analysis of repeated samples and lab standards.

5.2. Comparison with global temperature changes

Generally, SST variation in the northern SCS is quite comparable to global/northern hemisphere temperature changes (Fig. 4) (Ljungqvist, 2010; Mann, 2007; Moberg et al., 2005; PAGES 2k Consortium, 2013). Surface temperatures over the last two millennia are characterized with largely worldwide "Medieval

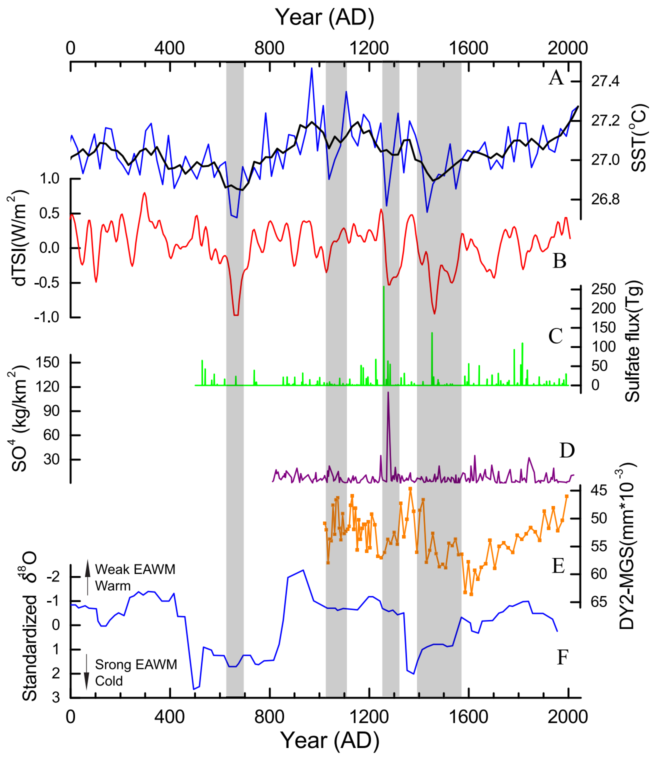

Fig. 4. Comparison of (A) NS02G-SST (black line is 5-points smoothing) with (B) ΔTSI (Steinhilber et al., 2009); (C) global volcanic stratospheric sulfate injection (Gao et al., 2008); (D) northern Hemisphere SO_4 flux (Crowley and Unterman, 2013); (E) DY2 mean grain size (MGS) on Dongdao of Xisha Islands (Yan et al., 2011); (F) standardized $\delta^{18}O$ of foraminifera *Neogloboquadrina incompta* in core SK-2 in the western North Pacific (Sagawa et al., 2014).

Warm Period" (WMP) and "Little Ice Age" (LIA). Though it is hard to define the time span of MWP and LIA periods at multi-decadal scale because of broad regional heterogeneity (PAGES 2k Consortium, 2013), these two concepts have been widely accepted to refer to a sustained warm interval of 9–13th century and a cold period of 15–18th century, respectively (Crowley, 2000; Mann et al., 2009). The NS02G-SST was slightly higher from ~900 to 1400 AD, with the warmest point at ~970 AD. It seems to match the global temperature peak at the time (PAGES 2k Consortium, 2013). The SST shows a slightly decreasing trend during 0-600 AD and 960–1400 AD, also quite in accordance with global temperature changes.

Several significant cooling events at 640-670 AD, 1030-1080 AD, and 1260-1280AD observed in the NS02G-SST record, seem to match with minor changes in the global temperature records. However it should be noted that synthesis of the global temperature might diminish the amplitude of some short-term changes because of complex variability in the data used. By comparing with another high resolution SST in the southern Okinawa Trough, good coincidence could be identified in the fast cooling or warming events at ~500, ~940, ~1060 and ~1670 AD (Wu et al., 2012), within chronological uncertainty. This suggests that the multi-decadal to centennial SST changes in the northern SCS are influenced by common forcings to the globe, or at least to the western Pacific Ocean.

5.3. Solar irradiance and volcanism

Solar irradiance and volcanism have been considered as important forcing to explain climate changes over the last millennium (Crowley, 2000). The total solar irradiance (TSI) reconstructed based on cosmogenic ^{10}Be in ice core (Steinhilber et al., 2009) were compared with the NS02G-SST. The fluctuation patterns in SST and TSI exhibit a highly positive correlation through the last two millennia (Fig. 4). Higher SST usually corresponds to higher TSI, and most of the short-term cooling events coincides with TSI minima. This correlation thus suggests that the SST in the northern SCS is closely related to the solar irradiance energy.

Previous studies have suggested that alkenone-derived SST in tropical Pacific and Indonesian archipelago generally followed the increasing winter insolation through the Holocene (Leduc et al., 2010). The annual mean and January insolation at 20°N changed by −8 W/m^2 and ~20 W/m^2 respectively over the last 10 000 years (Laskar et al., 2004), corresponding to ~2 °C increase of $U_{37}^{K'}$-SST in the northern SCS (Wang et al., 1999a). Though still under debate, the $U_{37}^{K'}$ was considered to record annual mean SST, but with more weighted winter variability in tropical oceans (Popp et al., 2006; Schneider et al., 2010). In contrast, the TSI variability was less than 2 W/m^2 during the last 2 millennia, with corresponding NS02G-SST variability ~0.8 °C. Then, one question emerged: why the alkenone-derived SST was so sensitive to the TSI?

The straight-forward explanation might be ascribed to the direct modulation of solar irradiance to all seasonal insolation, consequently to the sea surface temperature. Alkenone-producing coccolithophores are living in the upper mixed layer in the ocean (Saavedra-Pellitero et al., 2014; Sun et al., 2011), thus could respond to solar energy-induced temperature changes very sensitively. Besides, the solar irradiance has been found in close relationship with the East Asian winter monsoon (EAWM) (Sagawa et al., 2014; Xiao et al., 2006), which exert great influence on the northern SCS SST (Kong et al., 2014). Sagawa et al. (2014) used the $\delta^{18}O$ of foraminifera *Neogloboquadrina incompta* to reflect the winter SST and winter monsoon intensity in the western North Pacific, revealed that the winter monsoon was stronger at 500-800 AD, 1350-1600 AD, weaker at 900-1300 AD, corresponding to the changes in NS02G-SST and TSI (Fig. 4). The standardized $\delta^{18}O$ show a weakening trend of EAWM since 1400 AD (Sagawa et al., 2014), in good agreement in the SST by this study. As the solar irradiance induced changes in the EAWM would cause SST warming/cooling in same direction as the TSI, the EAWM very likely have played a role in amplifying the TSI signals recorded in the SST.

However, some studies have proposed that volcanic eruptions had greater influence on millennia-scale climate than the solar irradiance (Schurer et al., 2014). Indeed, the abrupt cooling at ~1040, ~1270 and 1430 AD coincided with large amount of sulfate aerosol injection into the stratosphere via volcanic eruptions at 1024, 1258 and 1452 AD, respectively (Crowley and Unterman, 2013; Gao et al., 2008) (Fig. 4). Some minor cooling events, for instance, at ~1850 AD, also seem to relate to volcanic activities, despite of few years age differences (Crowley and Unterman, 2013).

Model simulations show that volcanic eruptions at 1258 AD and 1815 AD could lead to extra-tropical summer cooling by ~0.8–1.3 °C over the Northern Hemisphere land (Stoffel et al., 2015). Though volcanic eruptions cause less direct cooling over oceans than over lands (Man and Zhou, 2014), but could lead to strong and long-lasting adjustment of ocean dynamics, such as the Atlantic Meridional Overturning Circulation (AMOC) (Mignot et al., 2011). Weaker AMOC caused by decadally paced explosive volcanism may lead to Arctic Ocean sea ice expansion for >100 years during the LIA (Zhong et al., 2011), thus possibly intensify the Asian winter monsoon. In contrast, the Asian summer monsoon were found weaker during the following several years after volcanic eruptions (Man and Zhou, 2014; Zhuo et al., 2014), which could be also seen from the abrupt $\delta^{18}O$ increase at ~1260 AD in the Dongge Cave stalagmite (Dykoski et al., 2005).

In addition to the Asian monsoons, migration of the intertropical convergence zone (ITCZ) and Pacific Walker Circulation (PWC) were also thought to influence the climate in the SCS (Yan et al., 2011). Increased mean grain size (MGS) (Fig. 4) in a pond on the Xisha Islands suggest a wetter condition and perhaps westward shift of PWC during 1400-1850 AD (Yan et al., 2011), corresponding to lower SST in the NS02G. Within chronology uncertainties, short term cooling at 1200 AD and the recent 4-centuries warming seen from NS02G-SST are consistent with the DY2-MGS changes, implying possible connection between the northern SCS SST and PWC.

The alkenone-SST variation in the northern SCS might have recorded a complex combined effect of changed radiation energy, oceanic and atmospheric circulation. However it is hard to assess the contribution from each factor due to complicated interactions.

6. Conclusion

We have generated a bidecadal-resolution alkenone SST record over the last 2000 years from a gravity core NS02G in the northern SCS. The major findings are summarized below: (1) SST varied between 26.7 and 27.5 °C, with the range of ~1 °C; (2) Notable warm/cool periods could be identified during 900-1400 AD and 1400-1700 AD, coincident with the WMP and LIA periods, largely in agreement with northern hemisphere temperature records; (3) Short-term cooling events at 640-670 AD, 1030-1080 AD, 1260-1280 AD and 1420-1450 AD coincide with TSI minima and large volcanic eruption events, within chronological uncertainty. These findings suggest substantial impact of aerosol-induced forcing changes, as well as TSI changes, leading to atmospheric and ocean circulation changes and thus resulting in SST changes. However, chronological uncertainties and the data resolution from marine archives limit detailed association of SST changes with specific forcings.

Acknowledgement

This work was partially supported by the National Key Research and Development Program of China (2016YFA0601204), National Natural Science Foundation of China (41606070 and 41476010), HK RGC (HKU 707612P) and Foundation for Distinguished Young Teacher in Higher Education of Guangdong (YQ2014004). HKU research facility was supported by the Special Equipment Grant from the University Grants Committee of the Hong Kong Special Administrative Region, China (SEG HKU01).

Appendix A. Supplementary data

Supplementary data related to this article can be found at https://doi.org/10.1016/j.quaint.2017.10.001.

References

Anchukaitis, K.J., Breitenmoser, P., Briffa, K.R., Buchwal, A., Buntgen, U., Cook, E.R., D'Arrigo, R.D., Esper, J., Evans, M.N., Frank, D., Grudd, H., Gunnarson, B.E., Hughes, M.K., Kirdyanov, A.V., Korner, C., Krusic, P.J., Luckman, B., Melvin, T.M., Salzer, M.W., Shashkin, A.V., Timmreck, C., Vaganov, E.A., Wilson, R.J.S., 2012. Tree rings and volcanic cooling. Nat. Geosci. 5, 836–837.

Cobb, K.M., Charles, C.D., Cheng, H., Edwards, R.L., 2003. El Nino/Southern Oscillation and tropical Pacific climate during the last millennium. Nature 424, 271–276.

Conte, M.H., Sicre, M.-A., Rühlemann, C., Weber, J.C., Schulte, S., Schulz-Bull, D., Blanz, T., 2006. Global temperature calibration of the alkenone unsaturation index ($U^{K'}_{37}$) in surface waters and comparison with surface sediments. Geochem. Geophys. Geosyst 7, Q02005.

Crowley, T.J., 2000. Causes of climate change over the past 1000 years. Science 270–277.

Crowley, T.J., Unterman, M., 2013. Technical details concerning development of a 1200 yr proxy index for global volcanism. Earth Syst. Sci. Data 5, 187–197.

Dahljensen, D., Mosegaard, K., Gundestrup, N., Clow, G.D., Johnsen, S.J., Hansen, A.W., Balling, N., 1998. Past temperatures directly from the greenland ice sheet. Science 282, 268.

Dykoski, C.A., Edwards, R.L., Cheng, H., Yuan, D., Cai, Y., Zhang, M., Lin, Y., Qing, J., An, Z., Revenaugh, J., 2005. A high-resolution, absolute-dated Holocene and deglacial Asian monsoon record from Dongge Cave, China. Earth Planet. Sci. Lett. 233, 71–86.

Gao, C., Alan, R., Caspar, A., 2008. Volcanic forcing of climate over the past 1500 years: an improved ice-core-based index for climate models. J. Geophys. Res. Atmos. 113, 2036–2044.

Hu, J., Kawamura, H., Hong, H., Qi, Y., 2000. A review on the currents in the South China Sea: seasonal circulation, South China Sea warm current and Kuroshio intrusion. J. Oceanogr. 56, 607–624.

Kobashi, T., Kawamura, K., Severinghaus, J.P., Barnola, J.M., Nakaegawa, T., Bo, M.V., Johnsen, S.J., Box, J.E., 2011. High variability of Greenland surface temperature over the past 4000 years estimated from trapped air in an ice core. Geophys. Res. Lett. 38, 1440–1441.

Kong, D., Tse, Y.-Y., Jia, G., Wei, G., Chen, M.-T., Zong, Y., Liu, Z., 2015. Cooling trend over the past 4 centuries in northeastern Hong Kong waters as revealed by alkenone-derived SST records. J. Asian Earth Sci. 114 (Part 3), 497–503.

Kong, D., Zong, Y., Jia, G., Wei, G., Chen, M.-T., Liu, Z., 2014. The development of late Holocene coastal cooling in the northern South China Sea. Quat. Int. 349, 300–307.

Laskar, J., Robutel, P., Joutel, F., Gastineau, M., Correia, A.C.M., Levrard, B., 2004. A long-term numerical solution for the insolation quantities of the Earth. A&A 428, 261–285.

Leduc, G., Schneider, R., Kim, J.H., Lohmann, G., 2010. Holocene and Eemian sea surface temperature trends as revealed by alkenone and Mg/Ca paleothermometry. Quat. Sci. Rev. 29, 989–1004.

Liu, Y., An, Z., Linderholm, H.W., Chen, D., Song, H., Cai, Q., Sun, J., Tian, H., 2009. Annual temperatures during the last 2485 years in the mid-eastern Tibetan Plateau inferred from tree rings. Sci. China Ser. D-Earth Sci. 52, 348–359.

Liu, Z., Herbert, T., 2004. High-latitude influence on the eastern equatorial Pacific climate in the early Pleistocene epoch. Nature 427, 720–723.

Ljungqvist, F.C., 2010. A new reconstruction of temperature variability in the extra-tropical Northern Hemisphere during the last two millennia. Geogr. Ann. Ser. a-Phys. Geogr. 92A, 339–351.

Ljungqvist, F.C., Krusic, P.J., Brattstrom, G., Sundqvist, H.S., 2012. Northern Hemisphere temperature patterns in the last 12 centuries. Clim. Past 8, 227–249.

Müller, P.J., Kirst, G., Ruhland, G., von Storch, I., Rosell-Melé, A., 1998. Calibration of the alkenone paleotemperature index $U^{K'}_{37}$ based on core-tops from the eastern South Atlantic and the global ocean (60°N-60°S). Geochimica Cosmochimica Acta 62, 1757–1772.

Man, W., Zhou, T., 2014. Response of the East Asian summer monsoon to large volcanic eruptions during the last millennium. Chin. Sci. Bull. 59, 4123–4129.

Mann, M.E., 2007. Climate over the past two millennia. Annu. Rev. Earth Planet. Sci. 35, 111–136.

Mann, M.E., 2008. Proxy-based reconstructions of hemispheric and global surface temperature variations over the past two millennia. Proc. Natl. Acad. Sci. U. S. A. 105, 13252–13257.

Mann, M.E., Jones, P.D., 2003. Global surface temperatures over the past two millennia. Geophys. Res. Lett. 30, 1820.

Mann, M.E., Zhang, Z., Rutherford, S., Bradley, R.S., Hughes, M.K., Shindell, D., Ammann, C., Faluvegi, G., Ni, F., 2009. Global signatures and dynamical origins of the Little ice age and medieval climate anomaly. Science 326, 1256–1260.

Mignot, J., Khodri, M., Frankignoul, C., Servonnat, J., 2011. Volcanic impact on the Atlantic Ocean over the last millennium. Clim. Past Discuss. 7, 2511–2554.

Moberg, A., Sonechkin, D.M., Holmgren, K., Datsenko, N.M., Karlen, W., 2005. Highly variable Northern Hemisphere temperatures reconstructed from low- and high-resolution proxy data. Nature 433, 613–617.

Neukom, R., Gergis, J., 2012. Southern Hemisphere high-resolution palaeoclimate records of the last 2000 years. Holocene 22, 501–524.

Neukom, R., Gergis, J., Karoly, D.J., Wanner, H., Curran, M., Elbert, J., González-Rouco, F., Linsley, B.K., Moy, A.D., Mundo, I., 2014. Inter-hemispheric temperature variability over the past millennium. Nat. Clim. Change 4, 362–367.

Oppo, D.W., Rosenthal, Y., Linsley, B.K., 2009. 2,000-year-long temperature and hydrology reconstructions from the Indo-Pacific warm pool. Nature 460, 1113–1116.

PAGES 2k Consortium, 2013. Continental-scale temperature variability during the past two millennia. Nat. Geosci. 6, 339–346.

PAGES Ocean2k Working Group, 2012. Synthesis of marine sediment-derived SST records for the past 2 millennia: first-order results from the PAGES/Ocean2k project. In: AGU Fall Meeting. American Geophysical Union, p. PP11F-07.

Pelejero, C., Grimalt, J.O., 1997. The correlation between the $U^{K'}_{37}$ index and sea surface temperatures in the warm boundary: the South China Sea. Geochimica Cosmochimica Acta 61, 4789–4797.

Popp, B.N., Prahl, F.G., Wallsgrove, R.J., Tanimoto, J., 2006. Seasonal patterns of alkenone production in the subtropical oligotrophic North Pacific. Paleoceanography 21, 1–15.

Reimer, P.J., Bard, E., Bayliss, A., Beck, J.W., Blackwell, P.G., Ramsey, C.B., Buck, C.E., Cheng, H., Edwards, R.L., Friedrich, M., Grootes, P.M., Guilderson, T.P., Haflidason, H., Hajdas, I., Hatte, C., Heaton, T.J., Hoffmann, D.L., Hogg, A.G., Hughen, K.A., Kaiser, K.F., Kromer, B., Manning, S.W., Niu, M., Reimer, R.W., Richards, D.A., Scott, E.M., Southon, J.R., Staff, R.A., Turney, C.S.M., van der Plicht, J., 2013. Intcal13 and Marine13 radiocarbon age calibration curves 0-50,000 years Cal BP. Radiocarbon 55, 1869–1887.

Ruan, J., Xu, Y., Ding, S., Wang, Y., Zhang, X., 2015. A high resolution record of sea surface temperature in southern Okinawa Trough for the past 15,000 years. Palaeogeogr. Palaeoclimatol. Palaeoecol. 426, 209–215.
Saavedra-Pellitero, M., Baumann, K.-H., Flores, J.-A., Gersonde, R., 2014. Biogeographic distribution of living coccolithophores in the Pacific sector of the Southern Ocean. Mar. Micropaleontol. 109, 1–20.
Sagawa, T., Kuwae, M., Tsuruoka, K., Nakamura, Y., Ikehara, M., Murayama, M., 2014. Solar forcing of centennial-scale East Asian winter monsoon variability in the mid- to late Holocene. Earth Planet. Sci. Lett. 395, 124–135.
Schneider, B., Leduc, G., Park, W., 2010. Disentangling seasonal signals in Holocene climate trends by satellite-model-proxy integration. Paleoceanography 25, PA4217.
Schurer, A.P., Tett, S.F., Hegerl, G.C., 2014. Small influence of solar variability on climate over the past millennium. Nat. Geosci. 7, 104–108.
Shintani, T., Yamamoto, M., Chen, M.T., 2008. Slow warming of the northern South China Sea during the last deglaciation. Terr. Atmos. 19, 341–346.
Sicre, M.-A., Jacob, J., Ezat, U., Rousse, S., Kissel, C., Yiou, P., Eiríksson, J., Knudsen, K.L., Jansen, E., Turon, J.-L., 2008. Decadal variability of sea surface temperatures off North Iceland over the last 2000 years. Earth Planet. Sci. Lett. 268, 137–142.
Sikes, E.L., Volkman, J.K., Robertson, L.G., Pichon, J.J., 1997. Alkenones and alkenes in surface waters and sediments of the Southern Ocean: implications for paleotemperature estimation in polar regions. Geochimica Cosmochimica Acta 61, 1495–1505.
Smith, M., De Deckker, P., Rogers, J., Brocks, J., Hope, J., Schmidt, S., dos Santos, R.L., Schouten, S., 2013. Comparison of $U^{K'}_{37}$, TEX^H_{86} and LDI temperature proxies for reconstruction of south-east Australian ocean temperatures. Org. Geochem. 64, 94–104.
Steinhilber, F., Beer, J., Froehlich, C., 2009. Total solar irradiance during the Holocene. Geophys. Res. Lett. 36.
Stoffel, M., Khodri, M., Corona, C., Guillet, S., Poulain, V., Bekki, S., Guiot, J., Luckman, B.H., Oppenheimer, C., Lebas, N., Beniston, M., Masson-Delmotte, V., 2015. Estimates of volcanic-induced cooling in the Northern Hemisphere over the past 1,500 years. Nat. Geosci. 8, 784–788.
Su, J., 2004. Overview of the South China Sea circulation and its influence on the coastal physical oceanography outside the Pearl River estuary. Cont. Shelf Res. 24, 1745–1760.
Sun, J., An, B., Dai, M., Li, T., 2011. Live coccolithophores in the western South China Sea in summer 2007 (in Chinese). Oceanol. Limnologia Sinica 42, 170–178.
Volkman, J.K., Barrerr, S.M., Blackburn, S.I., Sikes, E.L., 1995. Alkenones in Gephyrocapsa oceanica: implications for studies of paleoclimate. Geochimica Cosmochimica Acta 59, 513–520.
Wang, L., Sarnthein, M., Erlenkeuser, H., Grimalt, J.O., Grootes, P., Heilig, S., Ivanova, E., Kienast, M., Pelejero, C., Pflaumann, U., 1999a. East Asian monsoon climate during the Late Pleistocene: high-resolution sediment records from the south China Sea. Mar. Geol. 156, 245–284.
Wang, L.J., Sarnthein, M., Erlenkeuser, H., Grootes, P.M., Grimalt, J.O., Pelejero, C., Linck, G., 1999b. Holocene variations in Asian monsoon moisture: a bidecadal sediment record from the South China Sea. Geophys. Res. Lett. 26, 2889–2892.
Wei, G., Deng, W., Liu, Y., Li, X., 2007. High-resolution sea surface temperature records derived from foraminiferal Mg/Ca ratios during the last 260 ka in the northern South China Sea. Palaeogeography, Palaeoclimatology. Palaeoecology 250, 126–138.
Wilson, R., Anchukaitis, K., Briffa, K.R., Büntgen, U., Cook, E., D'Arrigo, R., Davi, N., Esper, J., Frank, D., Gunnarson, B., Hegerl, G., Helama, S., Klesse, S., Krusic, P.J., Linderholm, H.W., Myglan, V., Osborn, T.J., Rydval, M., Schneider, L., Schurer, A., Wiles, G., Zhang, P., Zorita, E., 2016. Last millennium northern hemisphere summer temperatures from tree rings: Part I: the long term context. Quat. Sci. Rev. 134, 1–18.
Wu, W., Tan, W., Zhou, L., Yang, H., Xu, Y., 2012. Sea surface temperature variability in southern Okinawa Trough during last 2700 years. Geophys. Res. Lett. 39, L14705.
Xiao, S., Li, A., Liu, J.P., Chen, M., Xie, Q., Jiang, F., Li, T., Xiang, R., Chen, Z., 2006. Coherence between solar activity and the East Asian winter monsoon variability in the past 8000 years from Yangtze River-derived mud in the East China Sea. Palaeogeogr. Palaeoclimatol. Palaeoecol. 237, 293–304.
Xue, H., Chai, F., Pettigrew, N., Xu, D., Shi, M., Xu, J., 2004. Kuroshio intrusion and the circulation in the South China Sea. J. Geophys. Res. 109, C02017.
Yan, H., Soon, W., Wang, Y., 2015. A composite sea surface temperature record of the northern South China Sea for the past 2500 years: a unique look into seasonality and seasonal climate changes during warm and cold periods. Earth-Sci. Rev. 141, 122–135.
Yan, H., Sun, L., Oppo, D.W., Wang, Y., Liu, Z., Xie, Z., Liu, X., Cheng, W., 2011. South China Sea hydrological changes and Pacific Walker Circulation variations over the last millennium. Nat. Commun. 2, 293.
Zhao, M., Ding, L., Xing, L., Qiao, S., Yang, Z., 2014. Major mid-late Holocene cooling in the East China Sea revealed by an alkenone sea surface temperature record. J. Ocean Univ. China 13, 935–940.
Zhao, M., Huang, C.-Y., Wang, C.-C., Wei, G., 2006. A millennial-scale $U^{K'}_{37}$ sea-surface temperature record from the South China Sea (8°N) over the last 150 kyr: monsoon and sea-level influence. Palaeogeogr. Palaeoclimatol. Palaeoecol. 236, 39–55.
Zhong, Y., Miller, G.H., Otto-Bliesner, B.L., Holland, M.M., Bailey, D.A., Schneider, D.P., Geirsdottir, A., 2011. Centennial-scale climate change from decadally-paced explosive volcanism: a coupled sea ice-ocean mechanism. Clim. Dyn. 37, 2373–2387.
Zhuo, Z., Gao, C., Pan, Y., 2014. Proxy evidence for China's monsoon precipitation response to volcanic aerosols over the past seven centuries. J. Geophys. Res. Atmos. 119, 6638–6652.